

---

# A Novel Charged-Particle Diagnostic for $\rho R$ in Compressed ICF Targets

Areal density—the product of density and thickness of specific ions ( $\rho R$ ) in ICF targets—is an important measure of compression that enables a comparison of ICF implosions with simulation. In particular, this quantity influences several crucial aspects of an igniting target: the degree of self-heating in the target, its fractional burn, and gain.<sup>1</sup>

Several methods involving nuclear reaction products have been employed to deduce this quantity in ICF implosions.<sup>2–5</sup> In this article, we will discuss the use of knock-on particles (deuterons and protons) that have been elastically scattered from the 14-MeV primary DT fusion neutrons. Both knock-on deuterons<sup>2</sup> and protons<sup>5</sup> have been discussed previously in the literature. The knock-on deuteron diagnostic has been used extensively to provide a measure of  $\rho R$ .<sup>2</sup> The number of these knock-on particles can provide information on the areal densities of the layer in which they are produced, and the energy loss of these particles as they propagate out of the target will provide additional information about  $\rho R$  along the propagation path. The deuteron diagnostic can provide information about the compressed target in a relatively model-independent way for values of target  $\rho R$  up to  $\sim 100$  mg/cm<sup>2</sup>. For higher values of  $\rho R$ , the knock-on spectrum is significantly distorted and becomes very dependent on temperature within the target.

Maximum information from the knock-on diagnostics is obtained using detailed information about the shape and magnitude of the knock-on spectrum. Until recently, the technique used to detect the knock-on deuterons has involved the counting of tracks satisfying selective criteria in stacked track detectors, consequently providing only gross information about the particle spectrum. This lack of spectral information has limited the use of knock-on ions as a diagnostic. With the deployment of the new charged-particle spectrometer<sup>6</sup> (CPS), detailed spectral information of charged reaction products from the imploding target can now be obtained, enabling a more detailed analysis of conditions in the target using the knock-on particles. Using a 7.5-kG magnet, the CPS can momentum-select incident charged particles, which are then impinged onto a detector plane consisting of track detectors.

The identity of each particle is then established by comparing the track diameters with known stopping powers of various particles at that momentum. In this manner, areal densities can now be measured not only through the knock-on deuteron diagnostic but also through diagnostics involving other charged particles such as the knock-on protons.

The knock-on proton diagnostic is somewhat similar to the knock-on deuteron diagnostic. The number of these particles is once again proportional to the areal density of the layer in which they are produced (such as the plastic shell). The spectrum of these particles, however, is significantly different from the deuterons, and a different analysis must be used to interpret the measurement. In earlier work, a somewhat model-dependent technique to interpret the proton signal was presented.<sup>4</sup> A more model-independent analysis of the proton spectrum can be devised that relies on the number of knock-on protons in a suitably defined energy range and is equally applicable to current experiments. Details of this analysis will be presented elsewhere.<sup>7</sup>

Here we present a novel knock-on deuteron-based diagnostic that will simultaneously diagnose three regions of a compressed target consisting of DT gas enclosed in a CH shell overcoated by CD. This diagnostic is primarily based on measuring the knock-on deuteron spectrum and relies on knock-on protons for an independent measurement of the areal density of the plastic layers. Self-consistency would then dictate a favorable comparison between the values of the areal density of the CH layer inferred using the deuterons and protons.

In a direct-drive ICF target implosion, degradation in target performance is believed to occur primarily through Rayleigh–Taylor instability,<sup>8</sup> which is seeded by either target imperfections or laser nonuniformity. This instability, occurring at the ablation surface, can then feed through to the rear surface of the shell (or the fuel–pusher interface) during the acceleration phase of the instability. During the deceleration phase, these distortions at the fuel–pusher interface can grow, resulting in a mixing of the fuel and the pusher. The knock-on particle spec-

trum carries information about conditions in the target during this latter phase of the implosion. This is when core temperatures and densities are high enough to initiate the fusion process and to produce the knock-on ions. The mixing of the fuel and the shell at these times in the implosion can significantly modify the neutron production rate relative to one-dimensional (1-D) simulations and consequently the production of the knock-on ions and their spectra. Current diagnostics on the mixing of various layers in the target use x-ray spectroscopic signatures from various dopants in the target.<sup>9</sup> Techniques based on nuclear particles would provide an independent assessment of hydrodynamic mix in the target and could probe conditions in the target that are not easily accessible by x-ray spectroscopy. In addition, the knock-on deuteron diagnostic when used in conjunction with other diagnostic tools such as the neutron temporal diagnostic (NTD)<sup>10</sup> (which can measure the thermonuclear burn history of a target in an experiment) may serve to probe conditions in the compressed target at the onset of significant mix due to hydrodynamic instabilities.

In the sections that follow, we discuss (1) the knock-on particles from a typical target consisting of only two regions: DT fuel and a plastic (CH) shell. Knock-on deuterons (and tritons) are produced in the fuel, and knock-on protons are produced in the CH shell. (2) We then discuss specifically the knock-on diagnostic in the context of the elastically scattered deuterons and protons. (3) A generalization of this technique infers  $\rho R$  in three regions of the compressed target, using the detailed shape of the deuteron spectrum. The target involved has three layers: DT, CH and, CD. Knock-on deuterons are produced in both the DT and CD layers with two well-defined high-energy peaks in the spectrum, separated by an energy determined by the areal density of the intermediate plastic layer. Using the result from simulation as an example, we demonstrate the procedure for deducing the  $\rho R$  of the three layers from this spectrum. (4) We discuss how hydrodynamic instabilities could modify the measured knock-on deuteron spectrum and examine the validity of our analysis for these modified spectra. Finally, we mention briefly how we might compare our inferred results from experimental measurements to simulation.

**Knock-on Ions as a Diagnostic for  $\rho R$**

The knock-on diagnostic relies on the elastic scattering of various ions (deuterons and protons) in the target from the 14.1-MeV primary DT neutrons (Fig. 77.17). The number of such elastically scattered particles,  $N_K$ , is then proportional to the number of primary neutrons,  $Y$ , the number density for the

particle of interest,  $n_K$ , the average distance that the neutron traverses in the target,  $\langle R \rangle$ , and is given by

$$N_K = n_K \langle R \rangle \sigma_K Y, \tag{1}$$

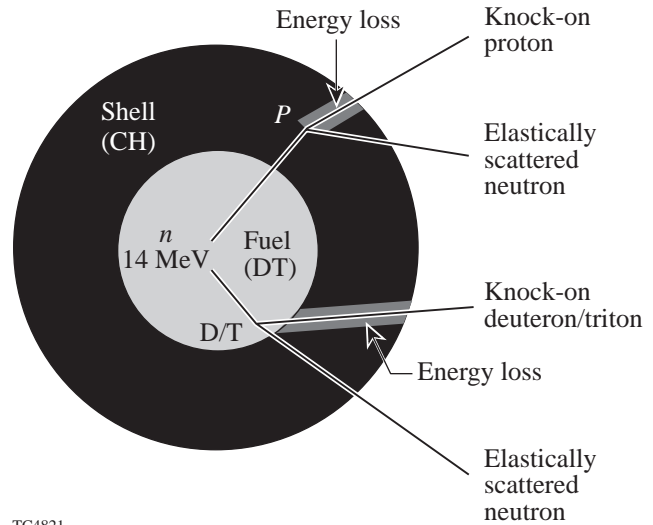
where the subscript  $K$  indicates the type of knock-on particle and  $\sigma_K$  is the corresponding cross section for elastic scattering (0.64b for deuterons and 0.69b for protons). Using the relation between the ion number density and the mass density, this can be rewritten for the number of knock-on deuterons produced in equimolar DT as

$$N_D = 7.7 \times 10^{-2} Y \langle \rho R \rangle \text{ cm}^2/\text{gm}, \tag{2}$$

where  $\langle \rho R \rangle$ , the areal density, is given by

$$\langle \rho R \rangle \equiv \int_0^R \rho dr. \tag{3}$$

The ratio of the number of knock-on deuterons to the number of 14.1-MeV DT primary neutrons provides a measure of the fuel's areal density. We note that knock-on tritons can also be produced in a similar elastic-scattering process with the energetic DT neutrons.



TC4821

Figure 77.17  
Knock-on process.

Knock-on protons may be produced by the addition of hydrogen to the fuel or from the protons in the plastic, if the target is prepared with a plastic shell. For knock-on protons produced from the plastic (CH) layer, Eq. (1) for the number of elastically scattered protons can be rewritten as

$$N_p = 3.2 \times 10^{-2} Y \langle \rho R \rangle \text{ cm}^2/\text{gm}. \quad (4)$$

Again, the ratio of the number of elastically scattered protons to the number of DT neutrons is proportional to the areal density of the plastic layer.

In an experiment, however, it is not possible to detect all the knock-on particles produced. The CPS has a finite solid angle and therefore samples only a fraction of the knock-ons produced. Therefore, an assumption about isotropy in knock-on production is required to infer the total number of knock-on particles produced. (Deviations from isotropy can be checked because there are two CPS's that view the target from different directions).

The more challenging aspect of inferring the number of knock-ons produced relates to the spectrum of these particles. The knock-on spectrum is produced over a continuum of energies extending over several MeV (knock-on deuterons occur up to 12.5 MeV, while the proton spectrum extends up to 14.1 MeV) due to different neutron-impact parameters. The entire spectrum cannot be measured because the very low-energy knock-ons can be stopped in the target or in the filter in front of the CPS. Also, the very high density of background tracks at lower energies makes the measurement of the entire spectrum challenging. As a result, these diagnostics rely on the identification of specific features of the knock-on spectra to deduce the total number of ions produced and hence the areal density of the layer of interest.

### 1. Knock-on Deuterons

Even though the entire knock-on deuteron spectrum cannot be measured, the number of knock-ons produced can be reliably deduced using the high-energy region of the spectrum. The anisotropic differential cross section for elastic scattering results in a clearly identifiable peak in the spectrum (shown schematically in Fig. 77.18). The number of deuterons under this peak is about 16% of the total number of deuterons produced in the scattering process and is relatively independent of any distortion of the spectrum that may occur due to the slowing down of the deuterons in the target for a large range of areal densities. This useful feature allows a model-indepen-

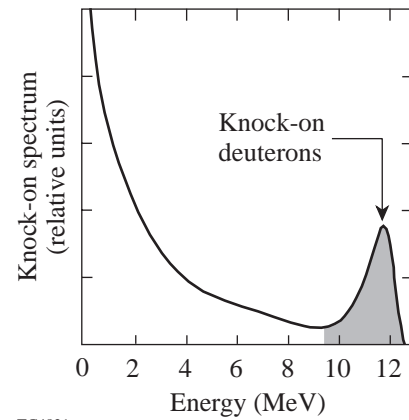


Figure 77.18  
Schematic spectra of the knock-on particles.

dent inference of the total number of knock-on deuterons produced [and hence the  $\rho R$  of the fuel,  $(\rho R)_f$  through Eq. (2)].

In addition to the fuel areal density, the knock-on deuteron spectrum can also provide a measure of the shell's  $\rho R$ . Knock-ons produced in the target slow down (primarily through energy loss in the shell), and as a result the spectrum is downshifted from its usual maximum of 12.5 MeV. Figure 77.19(a) shows the spectra due to different areal densities of the shell,  $(\rho R)_{CH}$ , calculated using a straight-line transport of the knock-on deuterons. The continuous energy loss of these charged ions is modeled using Ref. 11. The slowing down of the deuterons can be characterized by the end point of the spectrum (defined as the higher of the two energies of the half-maximum of the peak). As Fig. 77.19(b) indicates, this end point is proportional to the areal density of the shell, and this feature can be used to deduce this quantity in experiment.

An important feature of the knock-on deuteron diagnostic that enables a relatively model-independent measure of the shell's  $\rho R$  is the temperature insensitivity of the high-energy peak of the deuteron spectrum. Figure 77.20 shows the deuteron spectra for two different shell  $\rho R$  values at two different typical electron temperatures (the temperatures are typical of the shell in 1-D simulations of the implosions). Energy loss at these typical densities and temperatures in imploding ICF targets is dominated by losses to electrons (the electron density is related to the ion density and consequently the areal density of the material through its degree of ionization). Knock-on deuterons with energies greater than about 7 MeV typically have much higher velocities than electrons at the typical

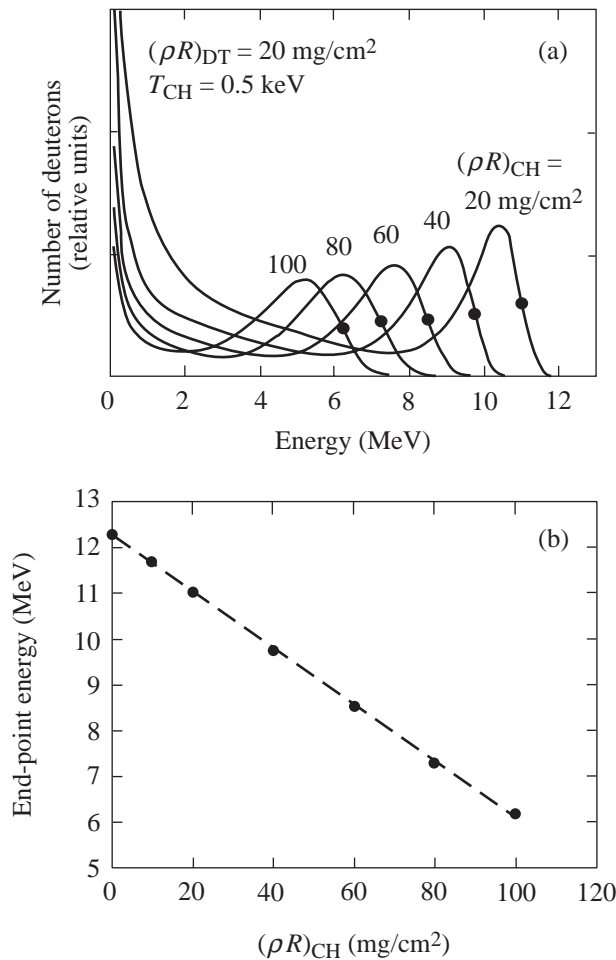


Figure 77.19 (a) The slowing down of the knock-on deuteron spectrum for different areal densities of the shell,  $(\rho R)_{CH}$ . (b) End-point energy of the spectrum as a function of the shell areal density.

temperatures in the cold plastic ( $\sim 0.5 \text{ keV}$ ). In this limit, the energy loss is independent of the electron's temperature and is thus dependent only on the shell's  $\rho R$ . As Fig. 77.19(a) indicates, for  $\rho R \geq 60 \text{ mg}/\text{cm}^2$ , the deuterons are slowed to less than 7 MeV. This value of  $\rho R$  suggests a limit on the maximum value of the shell's areal density that can be deduced independent of temperature considerations in the shell. On the other hand, the knock-on tritons, being more massive, show a greater sensitivity to both the temperature and the  $\rho R$  of the shell, limiting the range of temperatures and areal densities over which conditions in the target can be inferred reliably from their spectrum. However, the triton spectrum can be used as a self-consistency check on target conditions that have been measured by other diagnostics.

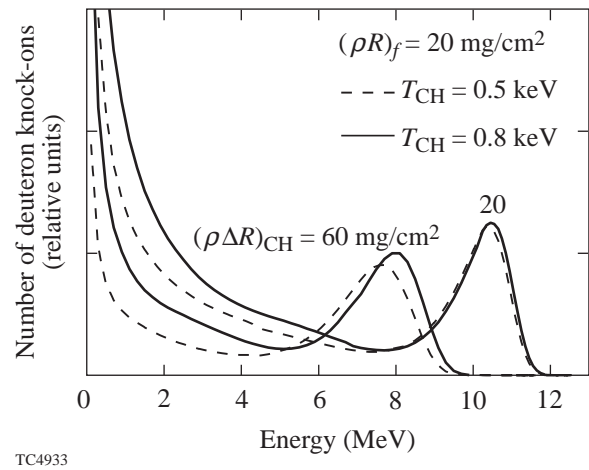


Figure 77.20 The deuteron spectrum is relatively insensitive to temperatures in the cold portions of the target.

Detailed knock-on spectra have been recently measured experimentally using the CPS. These preliminary spectra show good agreement with those obtained from simulations of implosions. In the next section, we consider a generalization of the knock-on deuteron diagnostic that will enable more detailed information about the compressed target.

### “Three-Layer” Targets

This extension of the deuteron diagnostic uses a target comprising three layers (shown in Fig. 77.21): an inner DT (or a DT+<sup>3</sup>He) fuel region, a plastic (CH) shell, and an ablator (CD). This target is different from those considered previously, where only two layers (DT and CH) were present. Its characteristics and dimensions are commensurate with targets surrogate to future cryogenic targets designed for the OMEGA laser,<sup>12</sup> and the diagnostic design permits some flexibility in each layer's thickness while retaining its equivalence to currently used surrogate targets.

Several energetic nuclear particles, shown schematically in Fig. 77.21, can be used to diagnose areal densities. Knock-on protons are produced in the plastic, and the areal density of the plastic layer can be deduced from the ratio of the number of protons produced to the number of primary neutrons. The addition of <sup>3</sup>He to the DT fuel is optional. The presence of <sup>3</sup>He in the target, however, provides another independent measure of areal density; the energy loss of the energetic 14.7-MeV proton from the D-<sup>3</sup>He reaction is proportional to the total areal density of the target.<sup>4</sup>

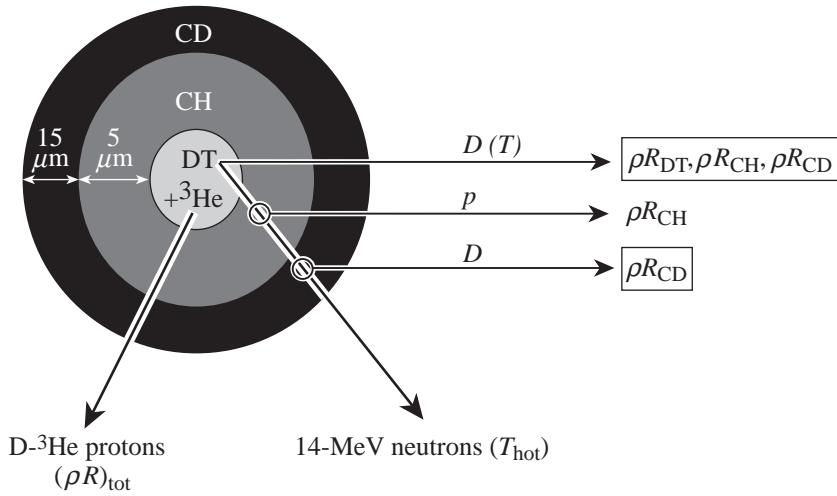
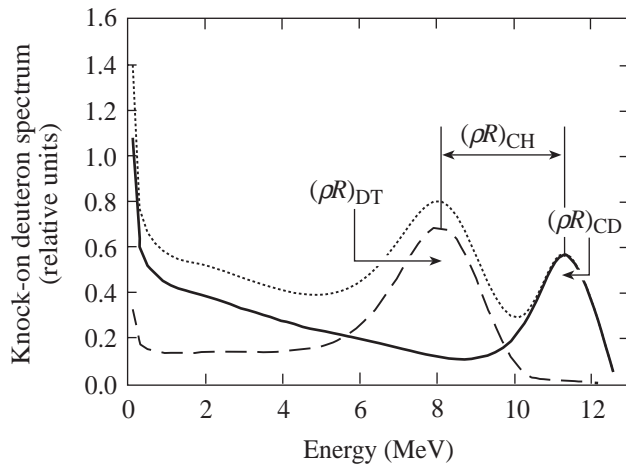


Figure 77.21  
Sources of particles for the diagnosis of areal densities in three-layer targets.

TC4844

Knock-on deuterons are produced in both the fuel and the CD layer. The deuterons produced in the fuel lose energy as they traverse the target, causing the high-energy peak to shift downward. The spectrum of deuterons from the CD layer, on the other hand, has its maximum energy at the nascent value of 12.5 MeV. The complete simulated spectrum for a target with a combined ablator and shell thickness of  $20 \mu\text{m}$  ( $5 \mu\text{m}$  CH and  $15 \mu\text{m}$  CD) is shown in Fig. 77.22. The target is driven with a 1-ns square pulse, which has been chosen arbitrarily. The spectrum is produced from a 1-D simulation of the implosion using the hydrodynamic code *LILAC*<sup>13</sup> and a post-processor that transports the knock-ons in straight lines for every time

step using the simulated density and temperature profiles while accounting for their energy loss. The relevant features are the two high-energy peaks in the spectrum arising from the individual contributions of the fuel and CD layers (shown as dashed lines in Fig. 77.22). The area under the higher-energy peak is primarily a measure of the areal density of the CD layer,  $(\rho R)_{\text{CD}}$ , whereas the peak at the lower energy has contributions from both the fuel and the CD shell. The separation of the two peaks provides a measure of the areal density of the plastic layer,  $(\rho R)_{\text{CH}}$ . We note that for the typical electron temperatures in the cold shell and ablator, the energy range spanned by the peaks of such a deuteron spectrum is fairly temperature insensitive. This temperature independence will be exploited later to deduce the areal densities of the three regions of the target from the data.



TC4845

Figure 77.22  
Simulated knock-on deuteron spectrum from a three-layer target with contributions from the individual layers.

The areal densities of the three layers can be deduced nearly model independently using the scheme outlined previously, if the peaks are well separated. We first consider the areal density of the plastic layer. For the spectrum shown in Fig. 77.23(a) (a solid line) the separation of the two high-energy peaks is about 3 MeV. The areal density of the plastic resulting in this separation should correspond to that value that results in a downshift of the end-point energy by the same amount. From Fig. 77.19(b), this separation corresponds to an areal density of about  $40 \text{ mg/cm}^2$  to be compared with the value of  $35 \text{ mg/cm}^2$  in the simulation. Next, to deduce the areal density of the CD layer, we calculate the total number of deuterons in the high-energy peak. This value is a known fraction of the total number of deuterons produced since this portion of the spectrum is unaffected by the presence of deuterons from the fuel. For the

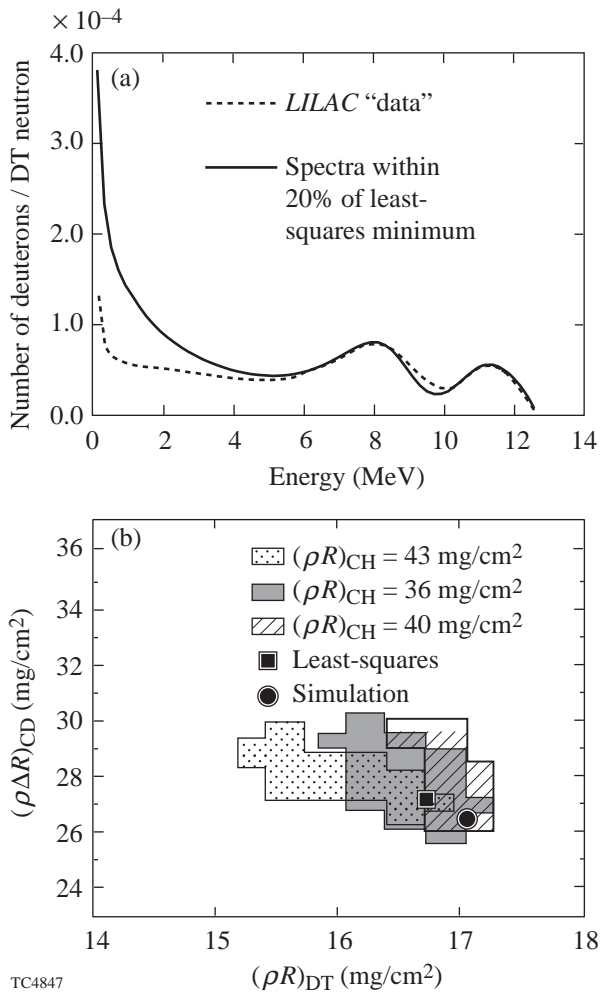


Figure 77.23 (a) Comparison of test (simulated) spectrum (solid line) showing spectrum from best-fit model (dashed line). (b) Areal densities for the three layers that result in spectra whose difference squared is within 20% of the least-squares value. Each shaded region represents the set of areal densities of the fuel and CD layer satisfying the 20% criterion, for a fixed value of the areal density of the CH layer.

spectrum (solid line) in Fig. 77.23(a), this is the number of deuterons above 10.25 MeV, and again, from the spectra in Fig. 77.19(a) this corresponds to about 12% of the total knock-on deuterons produced. Using this fraction for the number of deuterons in the peak and a formula for CD [similar to Eq. (2)], we obtain a value of 26.5 mg/cm<sup>2</sup> for the CD layer that compares favorably with the value of 25.6 mg/cm<sup>2</sup> in the simulation. While the areal densities of the CH and CD layers can be determined model independently, some uncertainty is introduced in the value of the areal density of the fuel,  $(\rho R)_f$ , since not all the deuterons under the low-energy peak are produced in the fuel. The contribution to this peak from the CD

layer depends on the slowing down of the deuterons and the geometry of the paths through the target. An upper limit for  $(\rho R)_f$  can be obtained by assuming that all the deuterons under this peak are produced in the fuel. In this case, the inferred areal density of the fuel using Eq. (2) is 23.6 mg/cm<sup>2</sup> to be compared with the simulation value of 17.0 mg/cm<sup>2</sup>.

This uncertainty in the value of the inferred fuel areal density can be mitigated through a different analysis of the knock-on deuteron spectrum. We consider deuteron spectra from a model where each layer is approximated by a constant density and temperature (an ice-block model). The density and the thickness of each layer are chosen by requiring a fixed mass for each layer (known from the specifications of the target being modeled) and a chosen  $\rho R$ . We note once again that since the deuteron spectrum is insensitive for the ranges of areal densities expected in such implosions, temperatures in the colder plastic and CD can be ignored in this analysis. The choice of fuel temperature, however, cannot be made arbitrarily since the deuterons may lose some energy in the hot fuel. In this example, we choose the fuel temperature at peak neutron rate in the simulation as the relevant fuel temperature. In deducing areal densities from the experimentally measured spectrum, the temperature obtained experimentally from the width of the DT neutron spectrum<sup>14</sup> (measured through time-of-flight techniques) should be used in the model.

In this manner we construct a static representation of the target and fit the spectra from such a model by varying the areal densities of each layer. While the ice-block model is not expected to accurately describe the primary complexities of an imploding target such as the spatial and time-dependent variation of densities and temperatures, the spatial localization of neutron sources in the target, and the geometry of the knock-on trajectories through the target, it should provide a reasonable time and spatially averaged representation of the target relevant to the knock-on spectrum.

To test our scheme for deducing the areal densities, we consider again the simulated spectrum shown as a solid line in Fig. 77.23(a). Using the model described above, we vary the  $\rho R$  of the three layers to minimize the least-squares difference between the spectrum from the model and the data. The energy range chosen for this minimization is the area determining the two peaks in the spectrum ( $\geq 5$  MeV). The technique for minimization we choose is based on the Downhill Simplex Method of Nelder and Mead.<sup>15</sup> If we assume that the neutrons are created uniformly in the fuel, the resulting spectrum of

such a minimization scheme is shown as the dashed line in Fig. 77.23(a). Our values for the areal densities for the DT, CH, and CD layers (16.5, 40, and 27.4 mg/cm<sup>2</sup>, respectively) compare favorably with the results from the simulation (17, 35, and 25.6 mg/cm<sup>2</sup>). These values agree very well with the model-independent extraction of the areal densities of the CH and CD layers, implying correctly well-separated peaks and, in addition, provide a tighter bound on  $(\rho R)_f$ .

To gauge the sensitivity of the spectrum to the least-squares values of  $\rho R$  obtained in this manner, we consider Fig. 77.23(b), which shows sets of  $(\rho R)_{CD}$  and  $(\rho R)_f$  for different values of  $(\rho R)_{CH}$ . [Each shaded region represents a set of areal densities of CD and fuel, corresponding to a certain value of  $(\rho R)_{CH}$ .] For each value of  $(\rho R)_{CH}$ , this set corresponds to those values whose spectra are within 20% of the least-squares value. This range of areal densities of CD and the fuel has been obtained by fixing the areal density of the plastic in the model to the required value and varying the areal densities of the CD and fuel layers. In this manner, we find the range of acceptable values of the areal densities of each layer in the target. Also shown in the figure is the least-squares value (square) and the result from the 1-D simulation (circle). We see that by using this procedure we obtain values of  $\rho R$  of the fuel and CD layer to within 10% of the true value. The larger range of acceptable values of  $(\rho R)_{CH}$  (35.5 to 43 mg/cm<sup>2</sup> for the plastic layer compared to 15 to 17.2 mg/cm<sup>2</sup> for the fuel and 25.5 to 29.1 mg/cm<sup>2</sup> for the CD layer) indicates that the deuteron spectrum is less sensitive to the areal density of the plastic layer. This is probably due to the fact that  $(\rho R)_{CH}$  does not determine an absolute number or energy; the relative separation of the two high-energy peaks is determined by this value. A comparison with the value deduced from the knock-on proton spectrum would, in addition, provide an independent check on the value of  $(\rho R)_{CH}$ . Finally, we note that the true set of areal density values obtained from the simulation is not excluded from our result at this 20% level, thus providing a measure of the sensitivity of the spectrum to the three areal densities.

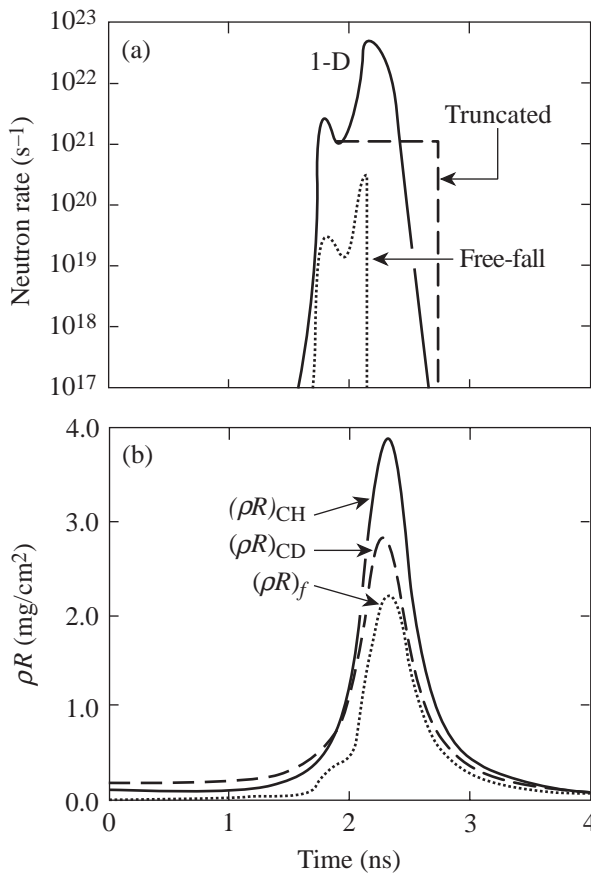
If we assume that the neutrons are produced in the center of the fuel and repeat the above analysis, we obtain the following results: an areal density of 16.3, 40.4, and 30.5 mg/cm<sup>2</sup> for DT, CH, and CD, respectively. The least-squares difference between the model spectra and the test data for this case is higher than for the uniform source ( $4.3 \times 10^4$  and  $2.1 \times 10^4$ , respectively), implying correctly a uniform distribution of the DT neutrons in the simulation.

### Modification of the Knock-on Deuteron Spectrum due to Mix

Our discussion has so far been based on a 1-D simulation of the implosion that does not include the effects of hydrodynamic instabilities and mix on the imploding target. In addition, any effects on the target due to long-wavelength asymmetries (possibly due to laser-beam imbalances in power and pointing errors) have also been ignored. The effects of such departures on nuclear and particle diagnostics are difficult to determine quantitatively from 1-D simulation.

During the deceleration phase, the Rayleigh–Taylor unstable fuel–pusher interface, seeded by its nonuniformity, can result in a mixing of the hot fuel and cold pusher. This mixing of materials at very different temperatures can result in a significant quenching of the neutron yield relative to 1-D simulations (that do not include this effect). Since the diagnostic should probe conditions in the compressed target corresponding to times of peak neutron and consequently knock-on production, this quenching can result in different conditions probed experimentally by the diagnostic relative to 1-D simulations. For the purposes of studying the feasibility of the diagnostic in the presence of such mixing, we assume that the effect of the deviations from 1-D is to exclusively change the neutron-production rate and hence the knock-on spectrum. In other words, the effect of such departures from 1-D behavior on the implosion dynamics is ignored.

To assess the effect of this mixing, we compare the spectra from purely 1-D simulations with two models of neutron rate truncation. These models should span the extremes of possible neutron rate truncations in the experiment. In the first model, we assume that a portion of the fuel implodes with a constant velocity acquired just before deceleration begins and is unaffected by the growing instabilities at the fuel–pusher interface. We then assume that the only neutron yield is from this portion of the fuel. The neutron rate from this model is shown in Fig. 77.24(a) as the free-fall rate and is significantly lower in magnitude relative to the 1-D simulation. Figure 77.24(b) shows the corresponding areal densities in the target from the simulation. As Figs. 77.24(a) and 77.24(b) indicate, the neutron rate in this model peaks earlier and thus probes earlier times in the implosion. This results in a deuteron spectrum (dotted line in Fig. 77.25) that is characteristic of smaller areal densities for all three layers. Our analysis provides values that agree reasonably with the results from simulation; the least-squares values are 9.8, 22.5, and 17.1 mg/cm<sup>2</sup>, whereas the results of the simulation are 8.9, 26.7, and 15.8 mg/cm<sup>2</sup>. We once again note that the independent measurement of  $(\rho R)_{CH}$



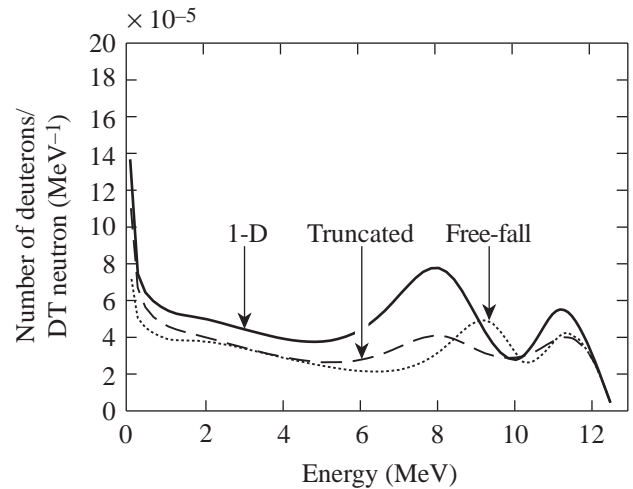
TC4934

Figure 77.24

(a) Neutron rate curves for different models used for assessing the modification of the deuteron spectrum due to hydrodynamic mix: solid line—result of a 1-D simulation; dotted line—neutron rate obtained from a free-fall model (see text); and dashed line—neutron rate fixed to a constant value at a certain time. (b)  $\rho R$  history of the target from 1-D simulations. In the simulations, the diagnostic is sensitive to areal densities near peak neutron rates and consequently peak compression.

using the knock-on proton spectrum can constrain the areal density of plastic inferred from the deuteron spectrum. The favorable comparison between the values of the areal densities inferred from the diagnostic and the true values suggests that the areal densities can still be deduced reasonably were such a modified spectrum the result of a measurement.

In a different model, we assume that the neutron rate proceeds as given by the 1-D simulation up to a certain time, and, thereafter, it proceeds at a constant rate given by the rate at the chosen time. This is shown in Fig. 77.24(a) as the constant burn rate model. A comparison with Fig. 77.24(b) indicates that the diagnostic then probes the times corresponding to the steep



TC4935

Figure 77.25

Knock-on deuteron spectra using the three models of neutron rate truncation shown in Fig. 77.24(a).

changes in the areal density. The significant neutron rate for a large fraction of time over which these changes in areal density occur in the target results in a considerably broadened emergent spectrum with less well defined peaks (dashed line in Fig. 77.25), which are to be compared with the results of the simulation (10.7, 32.3, and 16.0 mg/cm<sup>2</sup>). Nevertheless, the least-squared values (8.9, 22.9, and 18.7 mg/cm<sup>2</sup>) compare favorably with the results of the simulation (17.9, 36.0, and 23.0 mg/cm<sup>2</sup>), suggesting that our analysis can be used to reliably infer the areal density of each of the layers, even when the peaks in the spectrum are less well defined.

Experimentally, the neutron rate history can be obtained through the neutron temporal diagnostic (NTD).<sup>10</sup> One method to compare the implosion with 1-D simulations could be as follows: The experimentally obtained neutron rate curve could be used to identify the times in the implosion probed by the diagnostic—the diagnostic probes times around the peak neutron burn rate. An identification of these times would allow us to calculate the areal densities of the three layers from the simulation. A comparison of these values with those obtained from the knock-on diagnostic would shed light on whether conditions in the experiment compare favorably with the 1-D simulation up to the time probed by the diagnostic. If the areal densities inferred from the diagnostic differ considerably from those in the simulation, this procedure will allow one to identify a time when mixing effects have already significantly influenced the fusion processes. Independent of any comparison with detailed hydrodynamics simulations, the areal densi-

ties deduced from the knock-on deuteron diagnostic should be nearly model independent and would provide information about the conditions in the target corresponding to times in the implosion identified using the NTD. Further, a comparison with detailed mixing models may enable the identification of conditions in the target that would result in the observed neutron rate curves and the inferred values of ( $\rho R$ ).

### Summary and Conclusions

In this article, we have presented a new diagnostic based on knock-on deuterons, which will simultaneously diagnose the areal densities in three different regions of the compressed ICF target. These targets have three layers (DT, CH, and CD), and the areal density of each of these layers can be inferred from the deuteron diagnostic. In addition, knock-on protons from the CH layer can be used to independently deduce the areal density of the plastic.

When used in conjunction with a detector that measures the neutron rate history of an implosion (NTD), the time in the implosion probed by this diagnostic can be identified. This will permit a more detailed comparison between the simulation and experiment.

We have also examined the modification of the knock-on deuteron spectrum due to departures from 1-D behavior such as mixing. We conclude that while the spectrum may be influenced significantly by such departures from 1-D behavior, our method for analyzing the experimental spectrum should still reliably infer the areal densities in the three layers. Detailed mixing models would be required, however, to make any inferences about the mixing process in implosions. Experiments to measure these spectra from an imploding target are currently underway, and the results will be presented elsewhere.

### ACKNOWLEDGMENT

This work was supported by the U.S. Department of Energy Office of Inertial Confinement Fusion under Cooperative Agreement No. DE-FC03-92SF19460, the University of Rochester, and the New York State Energy Research and Development Authority. The support of DOE does not constitute an endorsement by DOE of the views expressed in this article.

### REFERENCES

1. G. S. Fraley *et al.*, Phys. Fluids **17**, 474 (1974).
2. S. Skupsky and S. Kacenjar, J. Appl. Phys. **52**, 2608 (1981).
3. M. D. Cable and S. P. Hatchett, J. Appl. Phys. **62**, 2233 (1987).
4. Laboratory for Laser Energetics LLE Review **73**, 15, NTIS document No. DOE/SF/19460-212 (1997). Copies may be obtained from the National Technical Information Service, Springfield, VA 22161.
5. H. Nakaishi *et al.*, Appl. Phys. Lett. **54**, 1308 (1989).
6. D. G. Hicks, C. K. Li, R. D. Petrasso, F. H. Seguin, B. E. Burke, J. P. Knauer, S. Cremer, R. L. Kremens, M. D. Cable, and T. W. Phillips, Rev. Sci. Instrum. **68**, 589 (1997).
7. P. B. Radha and S. Skupsky, "A Novel Charged-Particle Diagnostic for  $\rho R$  in Compressed ICF Targets," in preparation.
8. Lord Rayleigh, Proc. London Math Soc. **XIV**, 170 (1883); G. Taylor, Proc. R. Soc. London Ser. A **201**, 192 (1950).
9. D. K. Bradley, J. A. Delettrez, R. Epstein, R. P. J. Town, C. P. Verdon, B. Yaakobi, S. Regan, F. J. Marshall, T. R. Boehly, J. P. Knauer, D. D. Meyerhofer, V. A. Smalyuk, W. Seka, D. A. Haynes, Jr., M. Gunderson, G. Junkel, C. F. Hooper, Jr., P. M. Bell, T. J. Ognibene, and R. A. Lerche, Phys. Plasmas **5**, 1870 (1998).
10. R. A. Lerche, D. W. Phillion, and G. L. Tietbohl, Rev. Sci. Instrum. **66**, 933 (1995).
11. S. Skupsky, Phys. Rev. A **16**, 727 (1977); J. D. Jackson, *Classical Electrodynamics*, 2nd ed. (Wiley, New York, 1975).
12. F. J. Marshall, B. Yaakobi, D. D. Meyerhofer, R. P. J. Town, J. A. Delettrez, V. Glebov, D. K. Bradley, J. P. Knauer, M. D. Cable, and T. J. Ognibene, Bull. Am. Phys. Soc. **43**, 1784 (1998).
13. E. Goldman, Laboratory for Laser Energetics Report No. 16, University of Rochester (1973).
14. H. Brysk, Plasma Phys. **15**, 611 (1973).
15. W. H. Press *et al.*, *Numerical Recipes in FORTRAN: The Art of Scientific Computing*, 2nd ed. (Cambridge University Press, Cambridge, England, 1992).